The Neuropeptide pth2 Dynamically Senses Others via Mechanosensation

Lukas Anneser[1], Ivan C. Alcantara[1,2], Anja Gemmer[1], Kristina Mirkes[1], Soojin Ryu[3], and Erin M. Schuman[1]

1: Max Planck Institute for Brain Research, Frankfurt, Germany

2: current address: Brown University, Providence, USA

3: Living Systems Institute & College of Medicine and Health, University of Exeter, Exeter, UK

First paragraph

Species that depend on membership in social groups for survival exhibit changes in neuronal gene expression and behavior when they face restricted social interactions or isolation[1–3]. Here we show that, across its lifespan, social isolation specifically decreased the transcription of the vertebrate-specific neuropeptide *pth2* in zebrafish, *Danio rerio*. Just 30 minutes of exposure to conspecifics, however, was sufficient to initiate a significant rescue of *pth2* transcript levels in previously isolated zebrafish. *Pth2* transcription exhibited bi-directional dynamics: following the acute isolation of socially-reared fish, a rapid reduction in *pth2* levels was observed. Curiously, *pth2* expression tracked not just the presence of others, but also their density. The sensory modality that controls *pth2* expression was neither visual nor chemosensory in origin, but rather mechanical - induced by the movements of neighboring fish. Chemical ablation of the mechanosensitive neuromasts within the fish's lateral line prevented the social-environment-induced rescue of *pth2* levels. In addition, mechanical perturbation of the water at frequencies similar to zebrafish tail movements was sufficient to rescue *pth2* levels in previously isolated fish. These data indicate a previously unappreciated role for a relatively unexplored neuropeptide, *pth2*, in both tracking and responding to the population density of an animal's social environment.

Although it is clear that varying social conditions can cause long-lasting changes in the behavior of fish, rodents, and primates[1,3,4], the brain systems associated with different types of social environment are not well understood. For example, while social isolation can modulate an animal's responsiveness to threats[5,6] and increases aggression[7], experiments probing the underlying molecular pathways have typically focused on small sets of candidate genes[5,8]. To assess to what extent neuronal genes respond to dramatic changes in the social environment, we raised zebrafish either alone (isolated) or with conspecifics (social) for different periods of time spanning larval and juvenile developmental stages (extended data fig. 1a). We performed next generation sequencing (NGS) on the global brain transcriptome of social and isolated fish and identified 319 genes that were either up- or down-regulated in isolated fish at 5, 8, 14 or 21 days post fertilization (dpf) (isolation began at 2 dpf; extended data fig. 1a, table S1, fig. 1a). Many transcripts exhibited isolation-induced regulation at a single time point, but 4 genes exhibited consistent isolation-induced down-regulation of gene expression across all ages examined (fig. 1a). Three of the transcripts (*egr1*, *fosab* and *npas4a*) were immediate early genes that respond to neuronal depolarization[9,10]. We thus focused our attention on the remaining transcript, *parathyroid hormone 2* (*pth2*), originally described as tuberoinfundibular peptide of 39 residues (TIP39)[11] a little-studied peptide that modulates maternal behavior[12], oxytocinergic signaling[13], and pain in rodents[14]. We validated the isolation-induced down-regulation of *pth2* transcripts at 5, 8 and 21 dpf using qPCR (fig. 1b). We noted that the isolation of zebrafish did not alter stress-related gene expression (extended data fig. 1, table S1). Since *pth2* is a member of a large gene family[15], we assessed the specificity of regulation and found that only *pth2*, and not other family members, responded to changes in the social environment

(extended data fig. 1b). Using an anti-pth2 antibody, we confirmed that isolation of zebrafish larvae also dramatically reduced pth2 protein levels (fig. 1c).

We used fluorescence in situ hybridization and immunolabeling to identify the cells that express *pth2*. As of 5 dpf, *pth2* is expressed in a bilateral cluster of 22 ± 3.7 cells in the dorsal thalamus[16] (fig. 1c and extended data fig. 2). Initially identified in hypothalamic extracts[17], rodent *pth2*-expressing neurons are found in the lateral pons and the thalamus[18] and project to[19,20] and regulate the hypothalamic pituitary axis[21]. In zebrafish, *pth2*-expressing cell bodies were localized at the lateral edge of the orthopedia transcription factor a (*otpa*) expression domain (extended data fig. 3a, b). *Otpa* regulates the specification of diencephalic neuroendocrine cells[22]. We used the juvenile (23 – 25 dpf) zebrafish brain single-cell RNA seq dataset of Raj et al.[23] and found that ~9% of neurons analyzed expressed the pth2 receptor[16], suggesting a broadscale influence of this neuropeptide (extended data fig. 4).

Does the effect of early social isolation result in long-lasting alterations in *pth2* levels or is *pth2* sensitive to the fish's current social environment? To address this, we first determined whether the isolation-induced decrease in *pth2* transcription could be rescued by the introduction of fish to a social context. Previously isolated (isolated from 2 to 5 dpf) fish were introduced to conspecifics in groups of 15 animals for 30 minutes, 1, 3 or 12 hours and then *pth2* transcripts levels were measured by qPCR. A brief (30 minute) exposure to conspecifics was sufficient to bring about a significant rescue of *pth2* transcript levels in previously isolated fish (fig. 2a). Following 3 hours with conspecifics *pth2* levels had reached 50% recovery and by 12 hours *pth2* levels were statistically indistinguishable from those observed in socially-reared animals (fig. 2a). The above data thus suggest that *pth2* levels reflect the current state of the fish's social environment.

Are *pth2* transcript levels still sensitive to isolation following rearing in a social environment? We found that the acute (6 hour) isolation of socially reared fish (5 dpf) brought about a significant decrease in *pth2* levels (fig. 2b). A similar pattern was observed when fish experienced prolonged rearing in a social environment until the juvenile stage (21 dpf) and then were isolated for 24 hours (fig. 2c). The *pth2* dynamics were observed throughout all developmental stages: raising zebrafish to adulthood in isolation (3 months) followed by a week in a social environment resulted in *pth2* levels that were indistinguishable from socially-reared fish (fig. 2d). Similarly, a life-long social rearing (3 months) followed by a week of isolation resulted in *pth2* levels that were indistinguishable from fish reared in isolation (fig. 2d). The sex of the animals did not have any effect on *pth2* expression in adult zebrafish (extended data fig. 5).

Given the acute sensitivity of *pth2* transcript levels to the presence of conspecifics, we next asked whether *pth2* levels reflect, quantitatively, the population density of the fish's environment. To address this, we raised fish (8 dpf) at densities of 1, 5, 20, 50, and 100 conspecifics per tank for 8 days and then measured *pth2* levels using qPCR. Over this broad range of conspecific densities, we found that *pth2* transcript levels were positively correlated with the number of fish present (fig. 2e).

Which sensory modality (or modalities) conveys information to the brain about the presence or absence of conspecifics? We first examined whether *pth2* levels were influenced by the chemosensory perception of others. The functionality of zebrafish chemosensation sensory systems has been demonstrated as early as 3 dpf, when animals display aversive behavior in response to chemical irritants[24] and a distinction between kin versus non-kin chemosensory cues has been observed at 6 dpf[25]. To test whether chemosensation participates in *pth2* rescue, we exposed isolated fish to

kin-imbued water (obtained from a 10-cm dish that housed 100 conspecifics) and measured the resulting *pth2* transcript levels. Transcript levels were unaffected by this treatment, indicating that chemosensation of conspecifics is not sufficient to rescue *pth2* expression (fig. 3a).

We next tested whether visual exposure to other zebrafish can influence *pth2* expression. Zebrafish respond to visual cues at 4 dpf[26] and begin visually-guided prey hunting at 5 dpf[27]. In these experiments, zebrafish (5 and 21 dpf) were placed in a chamber with two compartments separated by a transparent barrier, allowing the fish in one compartment to visualize conspecifics ("visual access") in the adjacent area. A previously isolated fish was placed in one compartment and socially-reared conspecifics were added to the adjacent, visually-accessible chamber. Following 3 hours in this chamber, there was no significant difference in *pth2* levels between isolated fish that were kept alone in their compartment and those that were given visual access to conspecifics (fig. 3b). The addition of conspecifics to the same compartment ("physical access") as the previously isolated fish, however, produced the expected increase in *pth2* levels. Moreover, adding six conspecifics to the adjacent chamber (visual access) in combination with five conspecifics in the same chamber (physical access) did not increase *pth2* levels further (fig. 3c), indicating that visual access does not govern the *pth2* transcript positive relationship with fish density (see fig. 2e). Finally, experiments in which animals reared in isolation were exposed to conspecifics in complete darkness, (a common procedure to investigate the contribution of visual cues[28]) exhibited a rescue of *pth2* levels. Taken together, these data indicate that visual experience does not affect the conspecific-induced regulation of *pth2* levels (fig. 3d).

Finally, we considered the possibility that information about the presence of conspecifics is conveyed via mechanosensation. Mechanical cues such as water flow have been shown to influence behavior of 5 dpf larvae[29]. Fish perceive water movement in their immediate vicinity via the lateral line[30], a sensory organ containing neuromast cells that are deposited along the side of the body. To test the necessity of mechanosensation, we ablated the lateral line with a short incubation in $CuSO_4$ or with neomycin, drugs that are routinely used to ablate neuromasts[31–35]. Ablation efficiency assessment with 4-(4-diethylaminostyryl)-N-methylpyridinium iodide (4-Di-2-ASP)indicated that all neuromast cells of the lateral line were absent or severely compromised, whereas the labeled cells in the olfactory epithelium remained intact (fig. 4a). In previously isolated animals (5 dpf) that underwent acute treatment to ablate the lateral line, exposure to conspecifics failed to induce an increase in *pth2* levels, suggesting that mechanosensation is required to regulate *pth2* levels (fig. 4b).

Can the isolation-induced reduction in *pth2* levels be rescued by mere mechanical stimulation of the water? To test this, we used brine shrimp (*Artemia salina*) which move with rhythmic strokes of their appendages[36]. We introduced artemia to previously isolated fish (5 dpf) for three hours and found that artemia, either in small numbers (~14) or in excess (~1000), did not induce *pth2* transcription. These data indicate that the mere displacement of the water was not sufficient to mimic the presence of conspecifics (fig. 4c). We next considered whether the mechanosensory circuits responsible for the detection of conspecifics are sensitive to particular features of larval zebrafish swimming behavior, including the frequency and timing of the mechanical stimulation. Zebrafish larvae swim in short, discrete bouts. During propulsion, their tails beat at frequencies of about 60-70 Hz[37]. We used a piezo actuator to deliver continuous 70 Hz vibrations to the water of previously isolated fish (5 dpf) and then examined *pth2* levels using qPCR. (We confirmed that neither the

presence of conspecifics nor the piezo movement significantly altered the global movement patterns of previously isolated fish (extended data fig. 6). Continuous stimulation at 70 Hz for 3 hours did not change *pth2* levels in previously isolated fish; the same stimulus paradigm delivered in kin-imbued swim water also failed to rescue *pth2* levels (extended data fig. 7a, b). In an effort to recapitulate the presence of multiple fish in a social environment and the fact that the mechanical stimulation associated with swimming is not continuous, we modified the piezo to include two arms with or without flexible appendages. We delivered the mechanical stimulation in discrete epochs (for 300, 500, 700, or 800 msec or 5 sec) with the same inter-stimulus intervals (in different experiments). None of these stimulation protocols brought about a *pth2* rescue in previously isolated fish (fig. 4d and extended data fig. 7b). We reasoned that the repetitive and predictable nature of the above stimuli likely differs from the variable patterns of water movement elicited by real conspecifics and could thus result in habituation in the isolated fish. We thus developed a paradigm in which both the duration of the mechanical stimulation and the inter-stimulus interval was chosen from a random distribution whose average corresponded to the mean duration of zebrafish tail movement and inter-bout intervals, respectively[37], validated by our own measurements of the kinematic features of freely swimming zebrafish larvae (extended data fig. 7c-f). We found that this less predictable pattern of mechanical stimulation resulted in a significant rescue of *pth2* levels in previously isolated fish (fig. 4d). As we observed with the rescue mediated by the presence of actual conspecifics, prolonging the duration of random stimulation further increased *pth2* levels (fig. 4d).

In other systems, the social environment can strongly modulate neuropeptide expression[2,33,38,39], resulting in behavioral and physiological plasticity. Isolation has been shown to affect the immune system[2,40] and the stress response[41] and several

brain regions, including the thalamus[7,41–43]. Here we found that gene expression of the neuropeptide *pth2* is tuned to changes in the social environment of the zebrafish throughout all developmental stages. We observed that *pth2* has a quantitative, rather than qualitative, relationship with the social setting of an animal, exhibiting expression levels that track conspecific density. In rats, *pth2*$^+$ cells project to oxytocinergic[14] and arginine-vasopressin$^+$ cells[22], two neuropeptides that regulate social behavior. Furthermore, the presence of *pth2* has been reported to regulate social behaviors such as rodent maternal care[14,20,36,37].

The mechanical cues that regulate *pth2* levels appear to be specifically tuned to swimming motion of conspecifics. There is growing evidence that social information can be transmitted via mechanical stimuli, e.g. as a means to mutually assess opponents before agonistic interactions in cichlids[46] or to induce gregarious behavior in locusts[47]. However, it is not known how neural circuits are influenced by social touch[30]. The dorsal thalamus, where we located the *pth2*$^+$ cells in zebrafish, receives input from the torus semicircularis, a structure that processes auditory cues and information from the lateral line[48], suggesting a potential pathway by which *pth2*$^+$ cells receive mechanosensory information. Considering that *pth2* expression is only increased by a specific stimulation pattern, it is noteworthy that regions adjacent to the mechanosensory integration site in the torus semicircularis are tuned to similarly distinct features in their stimulus domain: Specific responses to conspecific vocalizations have been described in the torus in both bony fish[49] and anurans[50]. Our results thus support the idea that mechanosensation is an important channel of social information[30]. It is clear that the presence of conspecifics can have dramatic consequences on an animal's access to resources and survival - it is thus likely that *pth2* secretion will regulate many neuromodulatory and behavioral networks.

205

206

1. Fulcher, N., Tran, S., Shams, S., Chatterjee, D. & Gerlai, R. Neurochemical and Behavioral Responses to Unpredictable Chronic Mild Stress Following Developmental Isolation: The Zebrafish as a Model for Major Depression. *Zebrafish* **14**, 23–34 (2017).

2. Slavich, G. M. & Cole, S. W. The Emerging Field of Human Social Genomics. *Clin Psychol Sci* **1**, 331–348 (2013).

3. Zelikowsky, M. *et al.* The Neuropeptide Tac2 Controls a Distributed Brain State Induced by Chronic Social Isolation Stress Article The Neuropeptide Tac2 Controls a Distributed Brain State Induced by Chronic Social Isolation Stress. *Cell* **173**, 1265-1268.e19 (2018).

4. Harlow, H. F., Dodsworth, R. O. & Harlow, M. K. Total social isolation in monkeys. *Proc Natl Sci USA* **54**, 90–97 (1965).

5. Kumari, A., Singh, P., Baghel, M. S. & Thakur, M. K. Social isolation mediated anxiety like behavior is associated with enhanced expression and regulation of BDNF in the female mouse brain. *Physiol. Behav.* **158**, 34–42 (2016).

6. Swerdlow, N. R. *et al.* Forebrain gene expression predicts deficits in sensorimotor gating after isolation rearing in male rats. *Behavioural Brain Research* **257**, 118–128 (2013).

7. Angulo, J. A., Printz, D., Ledoux, M. & Mcewen, B. S. *Isolation stress increases tyrosine hydroxylase mRNA in the locus coeruleus and midbrain and decreases proenkephalin mRNA in the striatum and nucleus accumbens*. *Molecular Brain Research* **11**, (1991).

8. Poletto, R., Siegford, J. M., Steibel, J. P., Coussens, P. M. & Zanella, A. J.

Investigation of changes in global gene expression in the frontal cortex of early-weaned and socially isolated piglets using microarray and quantitative real-time RT-PCR. *Brain Res.* **1068**, 7–15 (2006).

9. Yap, E. & Greenberg, M. E. Activity-Regulated Transcription : Bridging the Gap between Neural Activity and Behavior. *Neuron* **100**, 330–348 (2018).

10. Sun, X. & Lin, Y. Npas4 : Linking Neuronal Activity to Memory. *Trends Neurosci.* **39**, 264–275 (2016).

11. Usdin, T. B. Evidence for a Parathyroid Hormone-2 receptor selective ligand in the hypothalamus. *Endocrinology* **138**, 831–834 (1997).

12. Coutellier, L., Logemann, A., Rusnak, M. & Usdin, T. B. Maternal Absence of the Parathyroid Hormone 2 Receptor Affects Postnatal Pup Development. *J. Neuroendocrinol.* 612–619 (2011). doi:10.1111/j.1365-2826.2011.02149.x

13. Cservenák, M. *et al.* A thalamo-hypothalamic pathway that activates oxytocin neurons in social contexts in female rats. *Endocrinology* **158**, 335–348 (2017).

14. Dobolyi, A., Ueda, H., Uchida, H., Palkovits, M. & Usdin, T. B. Anatomical and physiological evidence for involvement of tuberoinfundibular peptide of 39 residues in nociception. *Proc. Natl. Acad. Sci. U. S. A.* (2002). doi:10.1073/pnas.042416199

15. Guerreiro, P. M., Renfro, J. L., Power, D. M. & Canario, A. V. M. The parathyroid hormone family of peptides : structure, tissue distribution, regulation, and potential functional roles in calcium and phosphate balance in fish. *Am. J. Physiol. Integr. Comp. Physiol.* **292**, R679–R696 (2007).

16. Bhattacharya, P., Yan, Y. L., Postlethwait, J. & Rubin, D. A. Evolution of the

vertebrate pth2 (TIP39) gene family and the regulation of PTH type 2 receptor (pth2r) and its endogenous ligand pth2 by hedgehog signaling in zebrafish development. *J. Endocrinol.* **211**, 187–200 (2011).

17. Usdin, T. B., Gruber, C. & Bonner, T. I. Identification and functional expression of a receptor selectively recognizing parathyroid hormone, the PTH2 receptor. *J. Biol. Chem.* (1995). doi:10.1074/jbc.270.26.15455

18. Cservenák, M. *et al.* Tuberoinfundibular peptide of 39 residues is activated during lactation and participates in the suckling-induced prolactin release in rat. *Endocrinology* **151**, 5830–5840 (2010).

19. Dobolyi, A., Cservenák, M. & Young, L. J. Thalamic integration of social stimuli regulating parental behavior and the oxytocin system. *Frontiers in Neuroendocrinology* **51**, 102–115 (2018).

20. Sugimura, Y. *et al.* Centrally Administered Tuberoinfundibular Peptide of 39 Residues Inhibits Arginine Vasopressin Release in Conscious Rats. *Endocrinology* **144**, 2791–2796 (2003).

21. Dimitrov, E. & Usdin, T. B. Tuberoinfundibular peptide of 39 residues modulates the mouse hypothalamic-pituitary-adrenal axis via paraventricular glutamatergic neurons. *J. Comp. Neurol.* **518**, 4375–4394 (2010).

22. Fernandes, A. M., Beddows, E., Filippi, A. & Driever, W. Orthopedia Transcription Factor otpa and otpb Paralogous Genes Function during Dopaminergic and Neuroendocrine Cell Specification in Larval Zebrafish. *PLoS One* **8**, e75002 (2013).

23. Raj, B. *et al.* Simultaneous single-cell profiling of lineages and cell types in the

vertebrate brain. *Nat. Biotechnol.* **36**, 442–450 (2018).

24. Vitebsky, A., Reyes, R., Sanderson, M. J., Michel, W. C. & Whitlock, K. E. Isolation and characterization of the laure olfactory behavioral mutant in the zebrafish, Danio rerio. *Dev. Dyn.* **234**, 229–242 (2005).

25. Gerlach, G., Hodgins-Davis, A., Avolio, C. & Schunter, C. Kin recognition in zebrafish: A 24-hour window for olfactory imprinting. *Proc. R. Soc. B Biol. Sci.* **275**, 2165–2170 (2008).

26. Brockerhoff, S. E. Measuring the optokinetic response of zebrafish larvae. *Nat. Protoc.* **1**, 2448–2451 (2006).

27. Neuhauss, S. C. F. Behavioral genetic approaches to visual system development and function in zebrafish. *J. Neurobiol.* **54**, 148–160 (2003).

28. Lloyd, E. *et al.* Evolutionary shift towards lateral line dependent prey capture behavior in the blind Mexican cavefish. *Dev. Biol.* **441**, 328–337 (2018).

29. Suli, A., Watson, G. M., Rubel, E. W. & Raible, D. W. Rheotaxis in larval zebrafish is mediated by lateral line mechanosensory hair cells. *PLoS One* **7**, (2012).

30. Butler, J. M. & Maruska, K. P. Mechanosensory signaling as a potential mode of communication during social interactions in fishes. *J. Exp. Biol.* **219**, 2781–2789 (2016).

31. Hernández, P. P., Moreno, V., Olivari, F. A. & Allende, M. L. Sub-lethal concentrations of waterborne copper are toxic to lateral line neuromasts in zebrafish (Danio rerio). *Hear. Res.* **213**, 1–10 (2006).

32. Groneberg, A. H., Herget, U., Ryu, S. & De Marco, R. J. Positive taxis and

299 sustained responsiveness to water motions in larval zebrafish. *Front. Neural*
300 *Circuits* **9**, 1–12 (2015).

301 33. Lush, M. E. & Piotrowski, T. Sensory hair cell regeneration in the zebrafish
302 lateral line. *Dev. Dyn.* **243**, 1187–1202 (2015).

303 34. Brown, A. D., Mussen, T. D., Sisneros, J. A. & Coffin, A. B. Reevaluating the
304 use of aminoglycoside antibiotics in behavioral studies of the lateral line.
305 *Hearing Research* **272**, 1–4 (2011).

306 35. d'Alençon, C. A. *et al.* A high-throughput chemically induced inflammation
307 assay in zebrafish. *BMC Biol.* **8**, 151 (2010).

308 36. Kirchner, S. R., Fedoruk, M., Lohmüller, T. & Feldmann, J. Analyzing the
309 Movement of the Nauplius 'Artemia salina' by Optical Tracking of Plasmonic
310 Nanoparticles. *J. Vis. Exp.* e51502 (2014). doi:doi:10.3791/51502

311 37. Müller, U. K. & Leeuwen, J. L. Van. Swimming of larval zebrafish : ontogeny of
312 body waves and implications for locomotory development. *J. Exp. Biol.* **207**,
313 853–868 (2004).

314 38. Pan, Y., Liu, Y., Young, K. A., Zhang, Z. & Wang, Z. Post-weaning social
315 isolation alters anxiety-related behavior and neurochemical gene expression in
316 the brain of male prairie voles. *Neurosci. Lett.* **454**, 67–71 (2009).

317 39. French, J. A., Taylor, J. H., Mustoe, A. C. & Cavanaugh, J. Neuropeptide
318 diversity and the regulation of social behavior in New World primates. *Frontiers*
319 *in Neuroendocrinology* **42**, 18–39 (2016).

320 40. Cole, S. W. *et al.* Myeloid differentiation architecture of leukocyte transcriptome
321 dynamics in perceived social isolation. *Proc. Natl. Acad. Sci. U. S. A.* **112**,

15142–15147 (2015).

41. Poletto, R., Steibel, J. P., Siegford, J. M. & Zanella, A. J. Effects of early weaning and social isolation on the expression of glucocorticoid and mineralocorticoid receptor and 11β-hydroxysteroid dehydrogenase 1 and 2 mRNAs in the frontal cortex and hippocampus of piglets. *Brain Res.* **1067**, 36–42 (2006).

42. Hermes, G., Li, N., Duman, C. & Duman, R. Post-weaning chronic social isolation produces profound behavioral dysregulation with decreases in prefrontal cortex synaptic-associated protein expression in female rats. *Physiol. Behav.* **104**, 354–359 (2011).

43. Robinson, S. A., Loiacono, R. E., Christopoulos, A., Sexton, P. M. & Malone, D. T. The effect of social isolation on rat brain expression of genes associated with endocannabinoid signaling. *Brain Res.* **1343**, 153–167 (2010).

44. Gellén, B., Zelena, D., Usdin, T. B. & Dobolyi, Á. The parathyroid hormone 2 receptor participates in physiological and behavioral alterations of mother mice. *Physiol. Behav.* **181**, 51–58 (2017).

45. Cservenák, M. *et al.* Thalamic neuropeptide mediating the effects of nursing on lactation and maternal motivation. *Psychoendocrinology* 3070–3084 (2013). doi:10.1016/j.psyneuen.2013.09.004

46. Butler, J. M. & Maruska, K. P. The mechanosensory lateral line is used to assess opponents and mediate aggressive behaviors during territorial interactions in an African cichlid fish. *J. Exp. Biol.* **218**, 3284–3294 (2015).

47. Simpson, S., Despland, E., Hägele, B. & Dodgson, T. Gregarious behavior in

desert locusts is evoked by touching their back legs. *Proc Natl Sci USA* **98**, 3895–3897 (2001).

48. McCormick, C. A. *Central Lateral Line Mechanosensory Pathways in Bony Fish*. *The Mechanosensory Lateral Line* (Springer-Verlag, 1989). doi:10.1007/978-1-4612-3560-6

49. Petersen, C. L. *et al.* Exposure to Advertisement Calls of Reproductive Competitors Activates Vocal-Acoustic and Catecholaminergic Neurons in the Plainfin Midshipman Fish, Porichthys notatus. *PLoS One* **8**, (2013).

50. Burmeister, S. S., Rodriguez Moncalvo, V. G. & Pfennig, K. S. Monoaminergic integration of diet and social signals in the brains of juvenile spadefoot toads. *J. Exp. Biol.* **220**, 3135–3141 (2017).

Fig. 1: Transcriptional response to social isolation.

a, Venn diagram showing the number of transcripts that were significantly (either up- or down-) regulated between the isolated and social groups. 319 mRNAs were regulated in total, but only 4 mRNAs were regulated in isolation groups of all durations (see table S1).

b, Box plots showing the validation of *pth2* as differentially expressed using qPCR. Dashed line indicates the level of *pth2* in socially reared fish at all time points. Expression of *pth2* is depicted relative to this value (independent qPCR replicates: 5 dpf = 7, 8 dpf = 4, 21 dpf = 6).

c, Coronal section from a confocal brain stack at the depth of the thalamus is shown (dorsal view, single frame). Visualization of *pth2* with in-situ hybridization and immunofluorescence labeling is only successful in socially reared fish (5 dpf). Scalebar equals 100 µm. Number of independent replicates = 5.

Fig. 2: Transcriptional dynamics of *pth2*.

a, *pth2* levels after increasing duration of social exposure in previously isolated fish (5 dpf). During social exposure, 15 animals were kept in a 10 cm dish in 45 mL E3. Transcript levels were normalized, 0 and 1 correspond to levels found in isolated and socially-reared fish, respectively. Purple shaded areas represent the standard deviation of isolated and socially reared fish. Values were compared to transcript levels of isolated fish (unpaired t-test, one-sided, BH-corrected: 30 minutes, $p_{(n=15,\ t=1.89)}$=1.3E-2, 60 minutes, $p_{(n=10,\ t=2.45)}$=5.4E-3, 3 hours, $p_{(n=10,\ t=4.95)}$=1.3E-5, 12 hours, $p_{(n=8,\ t=7.13)}$=1.4E-7). Values are reported as mean ± standard deviation.

b, Acute social isolation of socially reared fish (5 dpf, 15 fish per 10 cm dish). Animals were isolated for 3 or 6 hours, *pth2*-levels were normalized as in **a**). Values were compared to transcript levels of socially reared fish (unpaired t-test, one-sided, BH-corrected: 3 hours, $p_{(n=9,\ t=-1.04)}$=0.31, 6 hours, $p_{(n=3,\ t=-3.66)}$=5.8E-3). Values reported as mean ± standard deviation.

c, Impact of acute social isolation on juveniles. Socially reared fish (20 dpf) were placed in isolation for 24 hours. Transcript levels of *pth2* were indistinguishable from animals that were isolated since 2 dpf, indicated by the dashed line (n = 5 for all, paired t-test, one-sided, BH-corrected: 24 h isolation, $p_{t=-0.01}$=0.98, social, $p_{t=-23.6}$=3.8E-5).

d, Density-dependence of *pth2* levels in adults. Fish were raised to adulthood either in isolation or with conspecifics. After three months, isolated fish were exposed to conspecifics for one week (isolated + short soc.), socially reared fish were isolated for the same duration (social + short iso.). For isolated condition, n = 3, for all other n = 4 (unpaired t-test, one-sided, BH-corrected. Isolated vs isolated, short social: $p_{t=-5.49}$ =1.8E-3, social vs isolated, short social: $p_{t=-0.04}$ = 0.48, social vs social, short isolation – $p_{t=6.46}$=5.4E-6), isolated vs social, short isolation: $p_{t=6.46}$1.3E-3. Box plots in **c** and **d** represent the median (black line), the lower and upper quartile (box) with the whiskers indicating at most 1.5 x the interquartile range.

e, Dependence of *pth2* levels on number of conspecifics present. Animals were raised in different densities (1, 5, 20, 50, and 100 in 1.1 l tanks) until 8 dpf. Values reported as mean ± standard deviation.

Fig. 3: Sensory perception of conspecifics.

a, Box plots depicting the impact of chemosensory access to conspecifics on *pth2* levels. Expression levels are plotted in relation to isolated condition (dashed line). For all conditions, n = 3 (paired, one-sided t-test, BH-corrected. Medium swap: $p_{t=0.18}$=0.87, social rescue: $p_{t=-18.43}$=5.8E-3).

b, Scheme of forced visual access chambers and experimental results. Isolated fish (5 dpf, outlined in green) were of the Nacre (*mitfa*$^{-/-}$) phenotype and could thus be identified.

c, Box plots showing the *pth2* transcript increase in relation to isolated control fish (3c, top left, shown as dashed line) at 5 and 21 dpf. The impact of visual and physical access as well as the interaction of both was evaluated using a 2-way ANOVA. At 5 dpf, n = 5 for all groups. For visual access, $p_{F=3.21}$=0.09, physical access, $p_{F=53.94}$=2E-6, visual-physical interaction, $p_{F=2.93}$=0.11. At 21 dpf, n = 6 for all groups. For visual access, $p_{F=0.0002}$=0.99, physical access, $p_{F=30.64}$=2E-5, visual-physical interaction, $p_{F=0.60}$=0.44.

d, Box plots depicting the relative expression of *pth2* after three hours of social exposure either in darkness or under illumination as compared with an isolated control group (dashed line). For all groups, n = 6 (paired, one-sided t-test with BH-correction. For social exposure in darkness, $p_{t=7.59}$=9.5E-4, social exposure under illumination, $p_{t=10.04}$=5E-4, comparison between social exposure under illumination and in darkness, $p_{t=-1.42}$=0.22). Box plots in **b**, **d** and **e** represent the median (black line), the lower and upper quartile (box) with the whiskers indicating at most 1.5 x the interquartile range.

Fig. 4: Specific mechanosensation triggers transcription of *pth2*

a, Visualization of hair cells in the lateral line (white arrowheads) and the olfactory epithelium (grey arrowheads) in 5 dpf control fish and after treatment with neomycin or $CuSO_4$. Scale bar = 1 mm.

b, Box plots showing the impact of lateral line ablation on *pth2* levels after social exposure for three hours. Expression strength is plotted as compared to the isolated control group (dashed line). Paired, one-sided t-test with BH-correction. Under control conditions, $p_{(n=9,\ t=6.57)}$=5.2E-4, after $CuSO_4$ treatment, $p_{(n=5,\ t=1.39)}$=0.25, after neomycin treatment, $p_{(n=5,\ t=1.35)}$=0.25.

c, Box plots depicting the impact of different kinds of water disturbances on *pth2* levels, depicted as fold-changes as compared with the isolated control group (dashed line). Paired, one-sided t-test, BH-corrected, n=3 for all conditions. With 14 artemia, $p_{t=1.12}$=0.51, with approximately 1,000 artemia, $p_{t=-0.79}$=0.51, with 14 zebrafish, $p_{t=15.29}$=1.3E-2.

d, Box plots showing the impact of different stimulation paradigms on *pth2* transcript levels. Values are reported as compared to the isolated control condition (dashed line). Paired, one-sided t-tests, BH-corrected. For repetitive, regular stimulation of 300 ms intervals, n = 8 independent replicates $p_{(t=0.85)}$=0.42, for variable stimulation over three hours, n = 10 independent replicates, $p_{(t=3.76)}$=6.7E-3, for variable stimulation over six hours, n = 10 independent replicates $p_{(t=5.44)}$=1.2E-3. Box plots in **b**, **c** and **e** represent the median (black line), the lower and upper quartile (box) with the whiskers indicating at most 1.5 x the interquartile range.

Methods

Animal Stock and Husbandry

Adult and juvenile zebrafish of the lines Konstanz wildtype (KN) and Nacre (*mitfa*$^{-/-}$) were kept at 28°C on a light cycle of 14-hour light/10-hour dark and housed in 3.5 L ZebTEC tanks at a density of 5-35 fish of mixed sexes. Isolated fish and their socially-reared siblings were kept in 1.1 L tanks as of 6 dpf. Fish were fed with brine shrimp *(Artemia salina)* and/or GEMMA Micro three times per day. In addition, vinegar eelworms (*Turbatrix aceti*) were fed to larval and juvenile fish. Larvae up to 5 days post fertilization (dpf) were kept in dishes filled with E3 medium (5 mM NaCl, 17 mM KCl, 0.33 mM $CaCl_2$, 0.33 mM $MgSO_4$) in a 28°C incubator also in a 14-hour light/10-hour dark cycle. All animal procedures conformed to the institutional guidelines of the Max Planck Society and were approved by the Regierungspräsidium Darmstadt, Germany (governmental ID: V 54-19 c 20/15-F126/1016 and V 54-19 c 20/15- F126/1013).

Behavioral Experiments

Isolation of zebrafish

Batches of eggs were obtained from single pairs of adult zebrafish placed in a spawning tank overnight. Embryos were individually screened under a stereo microscope and deformed and dead embryos were removed. For isolation, animals were placed at 2 dpf individually in a 12-well dish filled with 3 mL E3. To prevent visual contact between larvae, opaque white paper strips were inserted between wells. For experiments with animals older than 5 dpf, fish were transferred at 6 dpf to a 1.1 L tank in a ZebTEC system containing artificial plants. Tanks were equipped with a grey plastic insert preventing visual access to surrounding tanks. For the socially-reared animals, fish were kept in a density-matched manner (1 fish per 3 mL

medium) in 10 cm dishes with 45 mL of E3. For experiments requiring animals older than 5 dpf, fish were transferred at 6 dpf to 1.1 L as described above. Unless specified otherwise, the social control group consisted of 5 fish per tank. In all experiments in which animals received access to conspecifics, siblings from the same batch were used, except for the experiments in which *mitfa*$^{-/-}$ fish were used to distinguish between treatment group and animals intended to serve as social stimuli.

Chemosensory access to conspecifics

To provide isolated fish with chemical access to conspecifics, dish medium was replaced by medium obtained from 10 cm dishes with 100 siblings in 45 mL E3. Medium was replaced every hour for three hours, after which time the fish were sacrificed. For direct comparison, previously isolated siblings were exposed to conspecifics in a 10 cm dish at a density of 15 fish in 45 mL E3 for three hours.

Visual access to conspecifics

Larvae isolated continuously from 2 dpf - 5 dpf were placed in one compartment of a dual compartment chamber with dimensions 1.5 x 3 x 1 cm³; adjacent compartments were separated by a transparent barrier made of plexiglass. For all conditions, fish were kept in one chamber for three hours. To provide visual access to conspecifics, 6 age-matched fish were placed in compartment adjacent to the previously-isolated fish. For physical access, 5 age-matched fish were placed together with the previously isolated fish in the same compartment. Pigmentation mutants (*mitfa*$^{-/-}$) were used to distinguish fish in these experiments.

Ablation of the lateral line

5 dpf previously isolated larvae were exposed to 50 µM CuSO4 for 10 minutes. CuSO4 was then washed out by exchanging the medium three times. Alternatively, animals were exposed to 100 µM neomycin for 5 minutes, followed by 3 medium

504 changes. Treated animals were then exposed to 14 untreated conspecifics (*mitfa*$^{-/-}$) in
505 a 10 cm dish (45 mL E3) for three hours.

506 **Exposure to artemia**

507 Previously isolated fish (5 dpf) were exposed to *Artemia salina* nauplii (either 14 or
508 ~1.000) in 10 cm dishes (45 mL E3) for three hours. Brine shrimp were obtained from
509 our in-house breeding culture.

510 **Measurement of zebrafish kinematic features**

511 Previously isolated fish were allowed to freely explore a small dish with a diameter of
512 10 cm filled with 45 mL E3 medium for 10 minutes. Recording took place using
513 acA2040-90uc camera (Basler) with a framerate of 20 fps at a resolution of 1.500 x
514 1.500 pixels. All recordings using Basler cameras were performed using the pylon
515 6.1.0 software. Using a custom-written python script, videos were background-
516 subtracted with a common Gaussian-Mixture segmentation algorithm. Features were
517 extracted using the OpenCV framework with parameters adapted for our setting. All
518 results were manually checked for accuracy.

519 **Free exploration task**

520 Animals that were either raised in isolation (2 – 5 dpf) or with conspecifics were
521 placed in a 10 cm dish either alone or with 14 conspecifics of a different phenotype
522 (*mitfa*$^{-/-}$). Fish at 5 dpf were allowed to explore the open field for 10 minutes, during
523 which they were recorded as described above. The video sample rate was 4 Hz.
524 Additional fish were evaluated at a later development stage (7, 14, 21, 28 dpf,
525 respectively) and placed in a rectangular chamber (2.4 x 7.6 cm) with an adjacent
526 compartment (0.6 x 7.6 cm) separated by a transparent barrier to assess the impact
527 of visual access to conspecifics on locomotion. Fish were allowed to explore the
528 chamber either in the presence or absence of age-matched conspecifics in the

adjacent compartment for 10 minutes. The Euclidean distance the animal moved between frames was used to compute the average velocity of the fish.

Mechanical stimulation

A piezo actuator (UPF-76Q-220, Ekulit) was placed in each well of a 12-well dish. Its vibration frequency was controlled via a frequency generator (AFG3102, Tektronix) after amplification of the signal using a custom-built amplifier. For most signals, the frequency generator was programmed to output 60 or 70 Hz continuously or in bursts of variable lengths (300, 500, 700, 800, 5000 ms) with a Vpp of 5.0. To generate more complex patterns, the frequency generator was set to an external trigger and gated using a TTL pulse delivered by an Arduino Mega 2560 Rev3 (Arduino). The Arduino board was controlled using a custom-written MATLAB script, which defined pause periods during which no stimulation was delivered by sampling from a log-logistic distribution ($\mu = 0.27$, $\sigma = 0.21$) and periods of activity during which the piezo was vibrating by sampling from a normal distribution ($\mu = 0.15$, $\sigma = 0.1$). Stimulation was delivered for three hours, unless otherwise specified in the main text. To assess the vibration pattern that was transmitted by the piezo to the well, we recorded a short video of the artificial mechanical stimulation paradigm described above. The sample rate was set to 180 Hz and recording took place for 60 seconds, using a BASLER acA1920-150uc. Time series data was extracted for pixels at the center of the dish near the piezo and at the edge of the dish, where water ripples were clearly visible after piezo activation. We applied a fast Fourier transform to convert the time series data to the frequency domain and verified that our stimulation produced water movement at the applied frequency throughout the dish.

After all experiments, animals were sacrificed in ice-cold water (0-4°C). Death was confirmed by the cessation of heart and gill movement.

Measurement of reactivity to piezo stimulation

To assess whether mechanical stimulation alters locomotor behavior, animals were tracked during the artificial stimulation paradigm as described above (in this setting, the camera was placed below the 12-well dish). From the tracked trajectories, we extracted the time points at which bouts were initiated and compared them with the onset of piezo activity to construct an event-triggered average.

RNA Isolation

For RNA isolation, whole heads were used from larvae and juveniles, while brains were extracted from adults. Per replicate, 10 to 15 heads were pooled for larvae and juveniles, while 2 brains were pooled for adult animals. Samples were collected on dry ice in RNase-free tubes and stored in 700 µL of TRIzol (ambion) either for immediate processing or storage for up to 3 days at 4 °C. Samples were homogenized using a 0.6 mm diameter needle attached to a 1 mL syringe. 140 µL of chloroform (Sigma-Aldrich) was added, and the tubes were vortexed for 15 seconds and centrifuged at 12,000 rcf for 15 minutes at 4°C. After phase-separation, 200 µL of the clear aqueous phase was obtained for RNA purification using the RNeasy MinElute Cleanup Kit (QIAGEN) according to the manufacturers' instructions. RNA was eluted in water and the concentration was measured using the NanoDrop. For NGS experiments, RNA quality was assessed using the Agilent 2100 Bioanalyzer system.

Real Time PCR

200 ng of RNA was used for reverse transcription using the QuantiTect Reverse Transcription Kit (QIAGEN) according to the manufacturer's recommendations. Dilutions (1:10) were used as template in the PCR. Each reaction contained 5 µL of

cDNA template, 1.3 µL primers, and 6.25 µL SYBR Green PCR master mix (Applied Biosystems). The cycling parameters used comprised an initial denaturation step at 95 °C for 10 minutes, followed by 40 cycles of denaturation (95 °C, 15 seconds) and amplification (60 °C, 60 seconds) on a Real Time PCR System (Applied Biosystems). The following primers were used for real time PCR: For *pth2*, 5'-CCACGCAACACACAGTCAAG-3' and 5'-GCAAGTTACTTTGCAGAGGTC-3', for *pth1a*, 5'-CTCTGAGAAGCAAACGGGCA-3' and 5'-GCTTCCCCTGGATACAGCTC-3', for *pth1b*, 5'-ATGCACCAGCTCCGAAACAT-3' and 5'-CCTCTTGCTAATTGGCAGTCCT-3', for *pth4*, 5'-GGAGAGCGAGAGTAGGCGT-3' and 5'-AGTGTGAAGCCCCTCAATGG-3', for *pthla*, 5'-CTGACGACGATCGTGAGGAC-3' and 5'-GCAAGGATCCAAATCTGTGGC-3', for *pthlb*, 5'-GCAGACAACGGCGTTCAGTC-3' and 5'-GTTTGGACACTCCCTTCGCT-3', for *tbp*, 5'-GTACTCACAGGTGCCAAGGT-3' and 5'-GATTGCGTAGGTCACCCCAG-3', for *StAR*[52], 5'- TCAAATTGTGTGCTGGCATT-3' and 5'-CCAAGTGCTAGCTCCAGGTC-3', and for *nr3c1*[52], 5'-ACAGCTTCTTCCAGCCTCAG-3' and 5'-CCGGTGTTCTCCTGTTTGAT-3'

The fluorescence threshold to be reached was set to 0.9 for all experiments and genes. For paired experiments, relative expression was computed by calculating the fold-change between control and experimental condition within each biological replicate. For unpaired experiments, relative expression was calculated in comparison with the mean value of the control condition. In all experiments, the ΔC_t method was used to compute these values[53].

Next-Generation Sequencing

200 ng of RNA was used for sample preparation with the TruSeq Stranded mRNA Kit (Illumina). Libraries were prepared according to the manufacturer's recommendations. In short, mRNA was enriched by selecting for poly-A-containing molecules using poly-T oligos attached to magnetic beads. mRNA was fragmented and primed with random hexamers to be converted to cDNA. AMPure XP beads were then used to purify double-stranded cDNA. A single A nucleotide was added to the 3'-end to enable the addition of i7 sequencing adapters. The incorporation of these specific sequences allowed for the identification of particular samples after sequencing. Libraries were purified, quantified using the Qubit 4 fluorometer (Invitrogen), and the average library size assessed with the Agilent HS DNA assay (Agilent). Equal amounts of all libraries were pooled and diluted to 4 nM in 10 mM Tris-HCl, ph 8.5, 0.1% Tween20. Equal amounts (5 µL) of library and 2 M NaOH were mixed and incubated for 5 minutes at room temperature to denature the DNA molecules. The mixture was neutralized by adding 5 µL of 200 mM Tris-HCl, pH 7.0. Denatured libraries were then diluted to 1.3 pM and loaded on a Mid Output Flow Cell (Illumina). Sequencing was performed on a NextSeq 500 machine (Illumina) using 151 sequencing cycles.

Gene Annotation and Analysis

Reads were mapped to the latest *Danio rerio* genome assembly (GRCz11) by utilizing the STAR algorithm[54]. Settings were adapted to exclude non-canonical intron motifs. Additionally, the options *--outFilterScoreMinOverLread* and *--outFilterMatchNminOverLread* were set to 0.25, respectively. The reads mapped to each gene were counted using the featureCounts algorithm with default options[55]. Genes were further annotated with the ENSEMBL gene ID, external gene name, description, GO-term, and entrezgene ID using the BioMart pipeline[56]. We used the

edgeR Bioconductor package to identify genes that were differentially expressed between fish reared in isolation and under social conditions[57]. Since our experiments were conducted in a paired manner (batches of full siblings were split and raised either isolated or under social conditions), our design matrix was formed based on an additive model incorporating batch identity and treatment, but without an interaction term, which is characteristic of paired designs. We estimated gene dispersion, fitted a linear model, and tested for the effect of different rearing conditions. The obtained p-values were corrected for multiple testing using the false-discovery rate correction method introduced by Benjamini and Hochberg[58].

Lateral line visualization

Hair cells in the lateral line were visualized by immersing live animals at 5 dpf in 50 µM 4-Di-2-ASP (Sigma-Aldrich) for 30 minutes. Medium was exchanged three times with fresh E3 before mounting the animals in agarose (1%). The effectiveness of the ablation was assessed using an Axio Zoom.V16 (Zeiss).

Whole-mount in-situ hybridization and immunohistochemistry

Fixation and staining were performed as described previously[59]. For visualizing *pth2*, we cloned a 1.1 kb fragment from cDNA using the primers 5'-GAAAGAGGCACCGTAGGCAA-3' and 5'-CTCTTCTGCTGGTGACCCAC-3' in a regular TA-cloning approach. A DIG-labelled riboprobe was synthesized following the instructions provided with the digoxigenin labeling mix (Roche, Nutley, NJ). The *otpa*-probe was generated by the Ryu lab. A custom antibody against *pth2* was produced using the epitope SQSQMEEELVKGWTGDWPSRVGHQQKR (Peptide Specialty Laboratories, Heidelberg, Germany). The antibodies against tyrosine hydroxylase and oxytocin were provided by Dr. Soojin Ryu[59,60]. The antibody against *znp-1* was acquired from Synaptic Systems (106002). All antibodies were used in a dilution of 1:500. After in-situ hybridization and immunohistochemistry, animals were transferred stepwise into 80 % glycerol and mounted dorsally for imaging using an inverted confocal microscope (LSM-780, Zeiss, Jena, Gemany). For all conditions, animals were imaged with a 20x air objective.

Registration to Z-brain

The stacks we obtained were co-stained with znp-1. Registration to the z-brain atlas was performed with the CMTK toolkit with standard settings[51,61]. For visualization of the cell clusters, cell bodies were manually annotated in a representative registered stack using the Fiji Multi-point tool[62] and overlaid with the Elavl3-H2BRFP[51] stack to visualize the zebrafish brain.

Modeling behavioral features

We used the behavioral data obtained from tracking individual fish to estimate features such as the interbout interval (IBI). Bouts were identified using the MATLAB function findpeaks, excluding local maxima that were not more than one standard

deviation over baseline. IBIs were measured as the time between peaks, slightly overestimating actual pause periods. The distribution underlying the IBIs was estimated with a log-logarithmic distribution. Bout lengths were estimated from published results with a normal distribution[63]. As for tail beat frequency, we chose 70 Hz as an average value reported for larval fish[37].

Data Analysis

Significance is reported as follows: * P<0.05, ** P<0.01, and *** P<0.001. Results are either reported as boxplots with individual data points overlaid or as mean ± sample standard deviation. In figure S2d, we highlighted only those individual data points outside 1.5 times the inter-quartile range. Whenever possible, a paired design was used by splitting the offspring of individual pairs of parents into different conditions that were processed together. All replicates reported are biological replicates obtained from different pairs of parents on different days. For NGS data, the statistical analysis is described in the corresponding section. For qPCR data, ΔCt values were obtained by normalizing Ct values of *pth2* or other genes of interest against the reference gene tbp. All ΔCt values are reported in the supplemental table S2. We tested for normality using data from figure 1d with the Shapiro-Wilk test and found that normality could be assumed. For paired designs, a one-sided, paired t-test was performed and corrected, if appropriate, for multiple tests with the Benjamini-Hochberg procedure. For unpaired experiments, a one-sided, unpaired t-test was conducted and likewise corrected. In fig. 3c, we conducted two separate 2-way ANOVA tests for each age group examining the influence of visual access to conspecifics, direct physical access to conspecifics, and the interaction between both variables. Since the interaction between both variables was not significant, we did not conduct further post-hoc tests. In extended Data fig. 6d, we conducted an ANOVA

693 incorporating all variables, resulting in the identification of age and rearing condition
694 as factors influencing animal velocity. Age was expected to induce an increase in
695 locomotion speed and was not further analyzed. Rearing condition was analyzed
696 using a one-sided post-hoc t-test corrected with Holm's method[64]. All data analysis
697 was performed using custom-written python (python 3.7) scripts in the jupyter
698 notebook 6.0.0 environment, embedded in the anaconda navigator 1.9.7 (64-Bit
699 version).

700

51. Randlett, O. *et al.* Whole-brain activity mapping onto a zebrafish brain atlas. *Nat. Methods* **12**, 1039–1046 (2015).

52. Alsop, D. & Vijayan, M. M. Development of the corticosteroid stress axis and receptor expression in zebrafish. *Am. J. Physiol. - Regul. Integr. Comp. Physiol.* **294**, (2008).

53. Livak, K. J. & Schmittgen, T. D. Analysis of Relative Gene Expression Data Using Real- Time Quantitative PCR and the 2−ΔΔCT Method. *Methods* **25**, 402–408 (2001).

54. Dobin, A. *et al.* STAR: ultrafast universal RNA-seq aligner. *Bioinformatics* **29**, 15–21 (2013).

55. Liao, Y., Smyth, G. K. & Shi, W. featureCounts : an efficient general-purpose program for assigning sequence reads to genomic features. *Bioinformatics* **30**, 923–930 (2014).

56. Durinck, S. *et al.* BioMart and Bioconductor: a powerful link between biological databases and microarray data analysis. *Bioinformatics* **21**, 3439–3440 (2005).

57. Robinson, M. D., McCarthy, D. J. & Smyth, G. K. edgeR: a Bioconductor package for differential expression analysis of digital gene expression data. *Bioinformatics* **26**, 139–140 (2010).

58. Benjamini, Y. & Hochberg, Y. Controlling the False Discovery Rate: A Practical and Powerful Approach to Multiple Testing. *J. R. Stat. Soc. Ser. B* **57**, 289–300 (1995).

59. Herget, U., Wolf, A., Wullimann, M. F. & Ryu, S. Molecular neuroanatomy and chemoarchitecture of the neurosecretory preoptic-hypothalamic area in

724 zebrafish larvae. *J. Comp. Neurol.* **522**, 1542–1564 (2014).

725 60. Ryu, S. *et al.* Orthopedia Homeodomain Protein Is Essential for Diencephalic
726 Dopaminergic Neuron Development. *Curr. Biol.* (2007).
727 doi:10.1016/j.cub.2007.04.003

728 61. Jefferis, G. S. X. E. *et al.* Comprehensive Maps of Drosophila Higher Olfactory
729 Centers: Spatially Segregated Fruit and Pheromone Representation. *Cell* **128**,
730 1187–1203 (2007).

731 62. Schindelin, J. *et al.* Fiji: An open-source platform for biological-image analysis.
732 *Nature Methods* **9**, 676–682 (2012).

733 63. Palmér, T., Ek, F., Enqvist, O., Olsson, R. & Åström, K. Action sequencing in
734 the spontaneous swimming behavior of zebrafish larvae - implications for drug
735 development. *Sci. Rep.* **7**, (2017).

736 64. Holm, S. A Simple Sequentially Rejective Multiple Test Procedure. *Scand. J.*
737 *Stat.* **6**, 65–70 (1978).

738 65. Raj, B., Gagnon, J. A. & Schier, A. F. Large-scale reconstruction of cell
739 lineages using single-cell readout of transcriptomes and CRISPR–Cas9
740 barcodes by scGESTALT. *Nat. Protoc.* (2018). doi:10.1038/s41596-018-0058-x

741

Acknowledgments

The authors would like to thank Stephanie Chanda, Jan Glüsing, Florian Vollrath and Claudio Polisseni for their contribution to the experiments, Anett-Yvonn Loos for her help with fish husbandry and discussions. The authors thank Gilles Laurent for discussions. S.R. and E.M.S are funded by DFG CRC 1193: Neurobiology of Resilience. E.M.S. is supported by the Max Planck Society.

Author contributions

L.A. and E.M.S. conceived the project. L.A., A.G., S.R., and E.M.S. designed the experiments. L.A., I.C.A., A.G., and K.M. conducted the experiments. L.A. wrote the code for data acquisition, analysis, and modeling. L.A. and E.M.S. wrote the manuscript.

Competing interests

The authors declare no conflict of interest. Correspondence and requests for materials should be addressed to E.M.S. Reprints and permissions information is available at www.nature.com/reprints.

Data Availability Statement

All data is provided in this paper or the accompanying Supplementary Information Files. All sequencing data has been made available under the SRA BioProject PRJNA627056. Gene annotation was performed using the publicly available ENSEMBL database (https://www.ensembl.org/Danio_rerio/Info/Index). The Z-Brain atlas can be downloaded from https://github.com/owenrandlett/Z-Brain[51]. Gene expression data from Raj et al.[23] are available under the Omnibus accession number GSE105010.

765

766 **Code Availability Statement**

767 All relevant code is available under the public

768 repository https://github.com/Anneser/SensingOthers/.

769

770

771 **Extended Data Fig. 1: Extended analysis of transcriptional responses to social**

772 **isolation**

773 **a,** Experimental scheme. Beginning at 2 dpf, larval zebrafish were raised in an

774 isolated or social (with four conspecifics) environment for 5, 8, 14 or 21 days. After

775 the specified periods, RNA was obtained from whole brains and next-generation

776 sequencing (NGS) was conducted. 6 replicates were obtained for 5 and 8 dpf, 5

777 replicates for 14 dpf, and 4 replicates for 21 dpf.

778 **b,** Box plots depicting the fold change of gene expression between isolated and

779 social groups (5 dpf) for all members of the pth-family in zebrafish. Only *pth2* shows a

780 significant change. Values are expressed relative to the isolated condition (n = 10 for

781 all experiments, paired t-test, one-sided, Benjamini-Hochberg-corrected: *pth2*,

782 $p_{t=9.82}<0.001$, *pthla*, $p_{t=-0.52}=0.62$, *pthlb*, *pth1a*, $p_{t=-2.55}=0.09$, *pth1b*, $p_{t=1.55}=0.31$, $p_{t=-}$

783 $_{0.92}=0.57$, *pth4*, $p_{t=0.51}=0.62$).

784

785 **c,** Gene expression data of previously described stress-responsive genes, *StAR*:

786 *steroidogenic acute regulatory protein*, adjusted p-value *; nr3c1: nuclear receptor*

787 *subfamily 3, group C, member 1; avp: arginine vasopressin*; *pomca*:

788 *proopiomelanocortin a*; *pomcb*: *proopiomelanocortin b*; and *oxt*: *oxytocin* (n = 6 for all

genes, FDR-corrected quasi-likelihood F-test implemented in edgeR, *StAR*: p = 0.99, *nr3c1*: p = 0.99, *avp*: p = 0.99, *pomca*: 0.99, *pomcb*: p = 0.99, *oxt*: p = 0.99).

d, Validation of gene expression analysis by qPCR for *StAR* and *nr3c1* after short exposure of previously isolated fish to conspecifics for 3 hours. Boxplots show expression relative to mean levels of isolated animals. Paired, one-sided t-tests, n = 6 for both genes. For *StAR*, $p_{t=0.37}$=0.71, for *nr3c1*, $p_{t=-0.45}$=0.66. Box plots in **b** and **d** represent the median (black line), the lower and upper quartile (box) with the whiskers indicating at most 1.5 x the interquartile range.

Extended Data Fig. 2: Registration and morphology of *pth2*$^+$ cells

a, Maximum-intensity projection (dorsal view) of the averaged Elavl3-H2BRFP stack from the z-brain atlas overlaid with the manually annotated position of *pth2*$^+$ cells.

b, Lateral view of the same stack.

c, Number of *pth2*$^+$ cells in each of the bilateral clusters. Stacks from 7 different 5 dpf larvae were counted. In the left cluster, 9.4 ± 2.4 cells were found, in the right one 10.9 ± 1.7 (mean ± standard deviation). Box plots represent the median (black line), the lower and upper quartile (box) with the whiskers indicating at most 1.5 x the interquartile range.

d, Depth-encoded (0 – 184 µm) Z-projection of whole-mount immunostaining against pth2 (5 dpf). White box shows area magnified in **e** – **g**.

e, Single frame on the level of the *pth2*$^+$ cell bodies.

f, Magnification of a single frame on the level of the posterior projections.

g, Single frame on the depth of the anterior projections of the *pth2*$^{+}$ cells, forming a dense neuropil in the telencephalon. Scale bar indicates 100 µm.

Extended Data Fig. 3: Localization of *pth2*$^{+}$ cells

a, *pth2*$^{+}$ cell bodies are forming bilateral clusters at the edge of the *otpa* domain in the diencephalon. More ventrally, cell projections were observed to closely appose the *otpa* domain and enter the telencephalon. 18 animals were imaged across 4 different experiments. All scale bars indicate 100 µm.

b, The *pth2*$^{+}$ cells are found dorsolateral relative to the main *TH*$^{+}$ cell clusters in the diencephalon. The rostral projections of the *pth2* clusters are found caudally to the telencephalic dopaminergic neurites. 14 animals were imaged across 3 different experiments.

c, *pth2*$^{+}$ cell bodies are slightly more dorsally located than the more rostrally situated *OXT*$^{+}$ neurons. Their telencephalic projections form a dense neuropil structure rostral to the neurosecretory hypothalamic preoptic area, where *OXT*$^{+}$ neurons are found. 4 different animals were imaged.

Extended Data Fig. 4: Evidence for widespread expression of *pth2r*

a, Clustering of cell types reproduced from Raj et al[65]. Data were used as provided under Gene Expression Omnibus accession number GSE105010 and analysed using the Seurat pipeline.

b, Distribution of *pth2r*-expressing cells. Grey points correspond to cells in which pth2r was not detected, the intensity of blue indicates how many reads were detected.

c, Distribution of *oxtr*-expressing cells.

d, Distribution of *avpr2aa*-expressing cells. Four receptors of *avp* were detected in the dataset, we show the one that was most widely expressed.

e, Barplots show the percentage of *pth2r*$^{+}$ cells within each cluster ("measured"). For each cluster, we also provide a bootstrapped estimation of what percentage would be expected by random sampling of cells, with numbers of bootstrapped cells being equal to cells belonging to the given cluster. In addition, we show the percentage of *pth2r*$^{+}$ cells across the entire population ("all")

f, Barplots show percentage of *avpr2aa*$^{+}$ cells within each cluster, same as in **e**. For *oxtr*$^{+}$ cells, not sufficiently many cells were identified in this dataset to perform this kind of comparison.

Extended Data Fig. 5: Impact of sex and density on *pth2* expression in adult zebrafish

a, Male and female adult zebrafish (3 mpf) were sampled from the same tank. Boxplots show *pth2* levels in relation to the mean level of male gene expression. Unpaired, one-sided t-test, $p_{(n=4,\ t=0.40)}$=0.69.

b, Boxplots show pth2 levels in adult zebrafish that were kept at densities of 5 and 35 per 3.5 l for one week, respectively. Expression levels were normalized to the mean level at the lower density. Unpaired, one-sided t-test, $p_{(n=6,\ t=2.44)}$=3.4E-2. Box plots in **a** and **b** represent the median (black line), the lower and upper quartile (box) with the whiskers indicating at most 1.5 x the interquartile range.

Extended Data Fig. 6: Impact of experimental conditions on locomotion

a, Boxplot shows the average velocity of 5 dpf animals that have been raised either in isolation or with conspecifics. Unpaired, one-sided t-test, n = 14 for isolation-reared fish, n = 11 for socially-reared fish, $p_{t=0.28}$=0.78.

b, Boxplot depicts average velocity of isolation-reared animals when swimming alone or together with 14 conspecifics. Unpaired, one-sided t-test, n = 8 for both conditions, $p_{t=0.32}$=0.75.

c, Scheme of the open field used in d. Animals were placed in a rectangular dish, which contained an adjacent compartment separated by a transparent barrier (indicated by dashed line), where (in some experiments) conspecifics were placed.

d, Boxplot shows the average velocity of animals at different developmental stages after rearing in isolation or with conspecifics. Visual access indicates whether conspecifics were placed in the adjacent compartment. An ANOVA revealed that visual access does not lead to differences between the groups ($p_{F=0.21}$=0.65). Speed increases with age ($p_{F=333.62}$=4.1E-47), and is influenced by raising condition ($p_{F=16.81}$=5.7E-5), although one-sided post-hoc t-tests corrected with Holm's method indicated no consistent influence on locomotion for the different age groups. Interaction effects were not observed. At 7 dpf without visual access (v.a.) and socially reared: N = 15, isolation-reared: N = 17, $p_{t=4.71}$=2.1E-4; N = 16 with v.a. and socially reared; N = 18 isolation-reared, $p_{t=2.38}$=6.9E-2; at 14 dpf without v.a., socially reared: N = 17 and isolation-reared: N = 16, $p_{t=1.55}$=0.19; with v.a. and socially reared N = 18 and isolation-reared N = 15, $p_{t=1.79}$=0.17; at 21 dpf, without v.a., socially reared: N = 18 , isolation-reared: N = 17, $p_{t=3.47}$=5.2E-3; with v.a. and socially reared N = 16 and isolation-reared N = 13, $p_{t=0.06}$=0.82; at 28 dpf, isolation-reared: N = 9 for

both cases, without v.a., socially reared: N = 15, $p_{t=0.23}$=0.82; with v.a. N = 18, $p_{t=2.25}$=8.3E-2. Box plots in **a**, **b** and **d** represent the median (black line), the lower and upper quartile (box) with the whiskers indicating at most 1.5 x the interquartile range.

e, Graph depicts the bout onset of larvae in response to piezo stimulation as explained in figure **4 d-e**. Bout onsets are displayed as relative frequencies, data from individual fish are shown in grey with the mean (smoothed with a rolling window of length 0.05 seconds) overlaid in purple.

Extended Data Fig. 7: Artificial mechanical stimulation

a, Experimental scheme for artificial mechanical perturbation. A randomized series of stimulation and pause periods was drawn from two distributions using a custom-written Matlab script. Periods of activity were propagated via an Arduino board to gate a frequency generator. The output signal was amplified before activating a piezo actuator transferring specific frequencies to a well in a 12-well dish with an isolated fish.

b, Scatter plot indicating *pth2* levels relative to isolated animals (dashed line) after 3 hours of different stimulation paradigms. Paired, one-sided t-tests with BH-correction were used. Single piezo element: for continuous stimulation, $p_{(n=6,\ t=-0.65)}$=0.54, for continuous stimulation in the presence of kin-imbued water, n = 2. Two piezo elements: for periodic stimulation at 300 ms intervals, $p_{(n=3,\ t=-0.18)}$=0.87, at 5 s intervals, n = 2. Two piezo elements with appendages: for periodic stimulation at 300

ms intervals, $p_{(n=3,\ t=-0.68)}$=0.57, at 500 ms intervals, n = 2, at 700 ms, $p_{(n=3,\ t=-0.82)}$=0.50, at 800 ms intervals, $p_{(n=5,\ t=-0.85)}$=0.44.

c, Larval zebrafish (5 dpf) were recorded for 10 minutes during a free exploration in 10 cm diameter dishes. Trajectories were used to extract behavioral features.

d, Locomotion of larval fish occurs in discrete bouts, facilitating the extraction of interbout-intervals (IBIs). In total, we extracted 16.326 IBIs from 25 fish.

e, Distribution of all IBIs is shown as a histogram, overlaid with a log-logarithmic distribution fit to the data.

f, Table displays all distribution types that were fitted to the IBI dataset and shows the corresponding Akaike information criterion.

Extended Data Fig. 8: Impact of genotype on *pth2* transcription

a) Boxplot shows the difference in *pth2* levels between socially reared and isolated Nacre (*mitfa*$^{-/-}$) larvae (5 dpf). 6 replicates were obtained, a paired, one-sided t-test showed that $p_{t=7.98}$=2.1E-4.

b) Same experiment as shown in fig 3d. Here, *pth2* levels of KN larvae were assessed and Nacre (*mitfa*$^{-/-}$) animals used as stooges. The impact of visual and physical access as well as the interaction of both was evaluated using a 2-way ANOVA. For all groups, n = 6. For visual access, $p_{F=0.83}$=0.37, physical access, $p_{F=144.96}$=1.3E-10, visual-physical interaction, $p_{F=2.41}$=0.14. Box plots in **a** and **b** represent the median (black line), the lower and upper quartile (box) with the whiskers indicating at most 1.5 x the interquartile range.

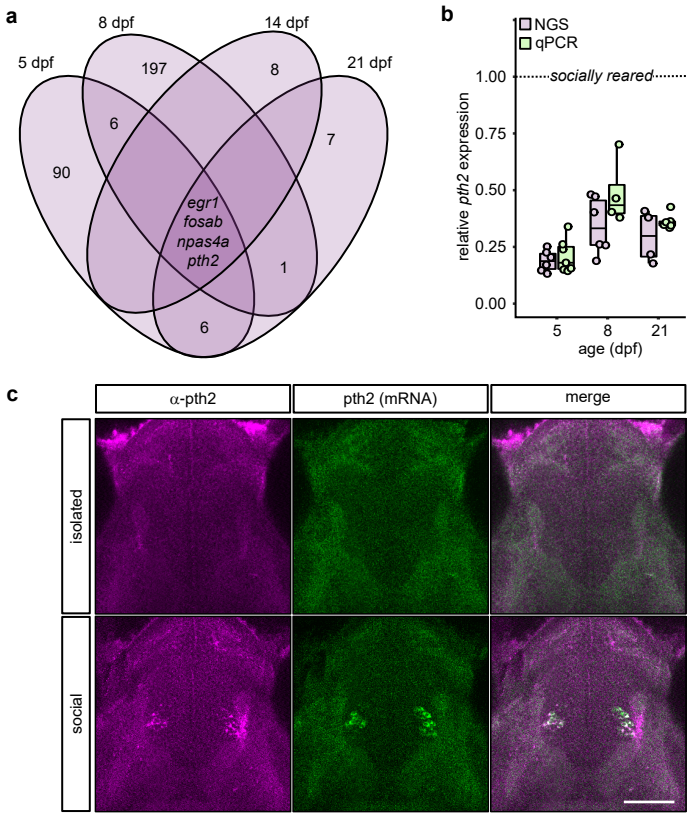
a
8 dpf
14 dpf
5 dpf
21 dpf
197
8
6
7
90
egr1
fosab
npas4a
pth2
1
6
b
NGS
qPCR
socially reared
1.00
0.75
0.50
0.25
0.00
relative pth2 expression
5
8
21
age (dpf)
c
α-pth2
pth2 (mRNA)
merge
isolated
social

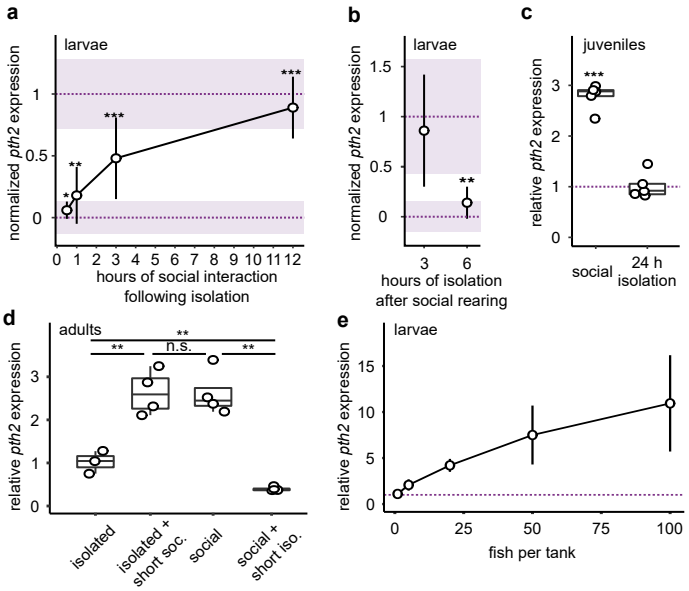
a
larvae
normalized pth2 expression
hours of social interaction
following isolation
b
larvae
normalized pth2 expression
hours of isolation
after social rearing
c
juveniles
relative pth2 expression
social
24 h
isolation
d
adults
relative pth2 expression
n.s.
isolated
isolated +
short soc.
social
social +
short iso.
e
larvae
relative pth2 expression
fish per tank

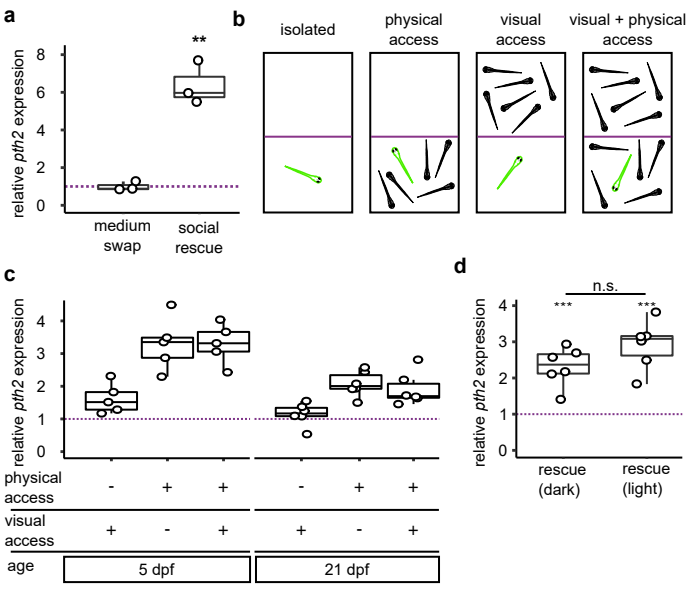
a
b
isolated
physical access
visual access
visual + physical access
relative pth2 expression
**
medium swap
social rescue
c
relative pth2 expression
physical access
visual access
age
5 dpf
21 dpf
d
n.s.
***
***
relative pth2 expression
rescue (dark)
rescue (light)

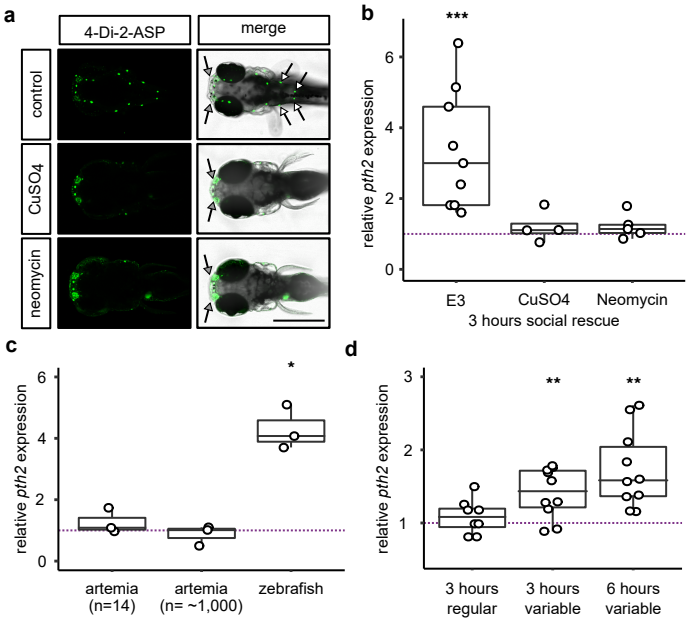
a
4-Di-2-ASP
merge
control
CuSO4
neomycin
b
***
relative pth2 expression
0
2
4
6
E3
CuSO4
Neomycin
3 hours social rescue
c
*
relative pth2 expression
0
2
4
6
artemia (n=14)
artemia (n= ~1,000)
zebrafish
d
**
**
relative pth2 expression
1
2
3
3 hours regular
3 hours variable
6 hours variable